

1 **Weak influence of paleoenvironmental conditions on the subsurface biosphere**
2 **of Lake Ohrid in the last 515 ka**

3

4 Camille Thomas^{1*}, Alexander Francke², Hendrik Vogel³, Bernd Wagner⁴, Daniel Ariztegui¹

5 ¹Department of Earth Sciences, University of Geneva, Geneva, Switzerland

6 ²School of Earth, Atmosphere, and Life Science, University of Wollongong, Wollongong, Australia

7 ³Institute of Geological Sciences & Oeschger Centre for Climate Change Research, University of Bern,
8 Bern, Switzerland

9 ⁴Institute of Geology and Mineralogy, University of Cologne, Cologne, Germany

10

11 Abstract

12

13 Understanding the response of geo- and biosystems to past climatic disturbance is primordial
14 to assess the short to long terms effects of current global change. Lacustrine sediments are
15 commonly used to investigate the impact of climatic change on biogeochemical cycling. In
16 these sediments, subsurface microbial communities play a primordial role in nutrient, organic
17 matter and elemental cycling, but they also can affect the sedimentary record and overprint
18 the original paleoenvironmental signal. Subsurface microbial communities have therefore
19 been investigated to assess the potential connection between microbial diversity and
20 environmental change. Lake Ohrid (North Macedonia, Albania) is the oldest lake in Europe
21 and has been the target of a scientific deep drilling in 2013. The upper 447 m of the 584-m-
22 long sedimentary drill core record obtained from the central part of the lake (DEEP site) is
23 composed of clayey to silty-clayey lithologies differing substantially in terms of carbonate and
24 organic matter content between glacials and interglacials. We investigated the microbial
25 diversity in the retrieved sediment using 16S rRNA gene sequences along the upper ca. 200 m
26 of the DEEP site record spanning ca. 515 ka to assess whether subsurface microbial
27 communities were following a similar trend.

28 Results show that *Atribacteria*, *Betaproteobacteria*, *Bathyarchaeota* and to a lower extent
29 *Dehalococcoidia* phyla structured the community but their occurrence appears to be
30 independent from each other. *Atribacteria* and *Bathyarchaeota* together with
31 *Dehalococcoidia* are commonly encountered in deep lacustrine and marine sediments. Their
32 metabolic versatility is adapted to low energy environments where they can realize the

33 fermentation of various substrates (sugars, propionate and amino acids). The generation of
34 H₂ from *Atribacteria* and other fermenters can be used by *Dehalococcoidia* and
35 *Bathyarchaeota* for acetogenesis, and even for chemolithoautrophic processes suggested at
36 greater depths. *Betaproteobacteria*-associated sequences were often co-occurring with
37 cyanobacterial sequences that suggest preservation of ancient DNA from the water column or
38 catchment, down to at least 340 ka. In particular, fossil DNA from *Cyanobacteria* in dry glacial
39 intervals may be the relict of ancient blooms of N-fixing clades in periods of nitrogen
40 depletion.

41 We compared the richness and diversity of all phlotypes with environmental parameters
42 measured in corresponding intervals to test for the relationship between paleoenvironmental
43 conditions, climatic modes and the subsurface biosphere. We found no significant relationship
44 between any phlotype and measured environmental parameters, nor with sediment age or
45 climate patterns. Our preliminary results support a weak recording of early diagenetic
46 processes and their actors by bulk prokaryotic sedimentary DNA in Lake Ohrid, which might
47 suggest dominant turnover and replacement by specialized low-energy clades of the deep
48 biosphere.

49

50 Keywords

51 *Bacteria, Archaea, Glacial stages, lake sediment, deep biosphere*

52

53 1. Introduction

54

55 With an age of at least 1.36 million years (Myr) [1], Lake Ohrid is considered to be the oldest
56 lake in Europe [1]. It is located at the border between North Macedonia and the Republic of
57 Albania. Owing to its age, location in the climate sensitive Mediterranean region and its high
58 degree of endemic biodiversity, Lake Ohrid has been targeted for a scientific deep drilling
59 campaign co-sponsored by the International Continental Scientific Drilling Program (ICDP) in
60 2013. Global and regional scale changes in Pleistocene glacial-interglacial climatic boundary
61 conditions exerted pronounced impacts on the terrestrial and aquatic environments in the
62 lake and its catchment [e.g. 1,2,11–13,3–10]. The main findings suggest that although
63 significant environmental changes are recorded in the catchment and the sediments [2,9], no
64 significant difference can be observed in terms of lake organisms diversification rates [14,15],

65 therefore concluding in a high resilience of the ecosystem in Lake Ohrid. In particular, diatom
66 communities were shown to quickly return to pre-disturbance state after significant tephra
67 fallout from volcanic eruptions (Campi Flegrei caldera) and did not experience evident changes
68 related to short-term climatic events (e.g. Heinrich H4 event) [15]. Similarly, diversification
69 rates of endemic microgastropods were quite constant and led Föller et al. (2015) to suggest
70 that the specific bathymetry, tectonic activity and karst hydrology of Lake Ohrid could buffer
71 environmental changes and contribute to the strong resilience of this ecosystem.

72 Among the organisms susceptible to respond to environmental change in lake systems,
73 prokaryotes have been the subject of increased attention in the past decade. Because Bacteria
74 and Archaea are present everywhere and are relatively sensitive to changes in organic matter
75 inputs, lake stratification, temperature, pH and salinity of lake systems [e.g. 17–19], the study
76 of their diversity in lake sediments has become a means to understand their long-term
77 response to environmental variations. In various lake systems, it has been shown that the
78 living deep biosphere was able to retain information on past climatic conditions [20,21]. In
79 particular, deep scientific drillings into lake sediments have advanced our understanding of
80 low energy systems and highly resilient subsurface microbial communities [22,23]. In Laguna
81 Potrok Aike (Argentina) for example, microbial communities and their imprint differed from
82 glacial to interglacial stages [24,25]. In Lake Van (Turkey), changes in sulfate reduction rates
83 were very sensitive to organic matter quality, varying as a function of changes in
84 environmental conditions [26]. In the hypersaline conditions of the Dead Sea, strong
85 similarities were observed between communities in sediments deposited in very arid
86 conditions, while sediments deposited during more humid periods displayed apparent
87 variability and diversified metabolic potential [27,28]. Such results, all originating from deep
88 scientific drilling projects, have shown that the deep biosphere is a precious tool to evaluate
89 and understand changes in paleoclimatic conditions, along with the variability it may cause in
90 diagenetic processes [29,30].

91 However, these results are still scarce, and more analyses from other lakes must be carried
92 out to validate and potentially generalize the hypothesis of retained sensitivity of the lake
93 subsurface biosphere to paleoclimatic conditions. Indeed, models and studies from other
94 lakes, generally in shallower sediments, have emphasized the strong dominance of low energy
95 taxa, similar to those found in ocean sediments [31]. A second hypothesis is therefore that
96 eventually conditions become too exclusive (i.e. poor in nutrients and in labile organic matter)

97 and result in the takeover of low energy organisms such as *Bathyarchaeota*, *Atribacteria*,
98 *Dehalococcoidia* or other microorganisms that are better adapted to the specificity of deep
99 sedimentary environments [31,32].

100 In order to test these hypotheses, we have explored the composition of 16S RNA gene
101 sequences from prokaryotic DNA in several sediment intervals along the DEEP site drill core
102 from the central part of Lake Ohrid. By comparing sedimentary microbial diversity and alleged
103 functions with environmental parameters associated to this sediment, we attempt to find links
104 and potential causality between the deep biosphere current structure, and chemical and
105 lithological characteristics of the sediment. We also compare this microbial composition with
106 the magnetic properties of the sediment, as previous work has emphasized a strong shift in
107 diagenetic paramagnetic minerals, likely caused by a change in microbial cycling in the
108 subsurface sediments of the lake [8]. Finally, we tested a link with climate simulation and
109 proxy observation data available for the past 1.36 Myr [1]. Studying the composition and
110 current functions of the deep biosphere of Lake Ohrid should allow deciphering if microbes
111 are more sensitive than eukaryotes to Quaternary changes in paleoenvironmental conditions,
112 or if the low energy environments of the deep subsurface along with buffer capacity of the
113 lake system has had a stronger impact and selected for adapted taxa, regardless of the original
114 conditions in the sediment.

115

116 2. Geological and limnological settings

117

118 Lake Ohrid covers an area of 358 km² at the border between Albania and North Macedonia
119 (Fig. 1A). It is located in a N-S extending pull-apart basin, between the Galicica (East) and
120 Mokra (West) mountain ranges (Fig. 1B), at an altitude of 693 m above sea level (asl). Its mean
121 water depth equals 150 m, with a maximum reached at 293 m. The lake is fed by karstic inflow
122 (55%, [33]), partly originating from neighboring Lake Prespa located 10 km east of Lake Ohrid,
123 small rivers, and direct precipitation on the lake surface. The high amount of nutrient poor
124 karst inflow results in an overall oligotrophic status of the lake.

125 The DEEP drilling site is located at 243 m water depth, in the central part of the lake
126 (41°02'57''N, 020°42'54''E, Fig. 1b). During the SCOPSCO drilling in 2013, several cores were
127 recovered at this site, reaching a terminal depth of 569 m below lake floor (mblf, [34]). The
128 upper 200 m of the DEEP site composite core analyzed herein is composed of a succession of

129 fine grained hemipelagic sediments, with a few (less than 5 cm-thick) intercalated event layers
130 classified as mass wasting deposits and tephra in the presence/absence of microscopic glass
131 shards [2,35]. Three lithotypes were identified in the fine-grained sediments, based on the
132 amount of calcium carbonate: calcareous silty clay, slightly calcareous silty clay and silty clay.
133 These variations are reflected in the calcite and total organic carbon (TOC) content of the
134 deposits. Silty clayey sediments are mostly characterised by low organic matter (OM)
135 concentrations, while OM can be moderate to high in calcareous and slightly calcareous
136 sediments. The sediments appear mottled or massive and lamination is absent, which implies
137 bioturbation and oxygenated bottom water conditions at the time of deposition [2].
138 In silty clay and slightly calcareous silty clay, TOC is predominantly of aquatic origin, as inferred
139 by the C/N ratio [36], while sediments from calcareous silty clay show C/N ratios occasionally
140 above 10, implying somewhat elevated terrestrial OM inputs. However, Francke et al. (2016)
141 suggest that these values may be affected by early diagenetic selective N loss, since the DEEP
142 site is almost completely disconnected to inlet stream supply. Rock-eval analyses on a Late
143 Glacial to Holocene sediment succession retrieved close to the Lini Peninsula (2.5 km to the
144 west of the DEEP site) revealed organic matter mainly of aquatic origin [10]. Lipid biomarker
145 analyses on sediments with similar age retrieved in close proximity of inlet streams however
146 yield dominance of terrestrial organic endmembers [37] which is also supported by C/N ratios
147 >10 in surface sediments close to the major inlets [38].
148 High diatom frustules content, high endogenic calcite concentrations, and overall high OM in
149 the core corresponds to periods of higher primary productivity, likely promoted by higher
150 temperatures and increased supply of nutrients and dissolved ions (Ca, CO₃) from the (karst)
151 catchment, i.e. conditions as they mainly occur during interglacial periods. On the opposite,
152 lower OM, endogenic calcite, and biogenic silica contents were interpreted as periods of lower
153 productivity, coupled with increased OM oxidation and mixing during the winter season
154 [2,5,13]. These conditions are primarily characteristic of glacial periods [2,13].

155

156 3. Material and methods

157

158 3.1. Sampling material

159

160 Samples for microbial and sediment biogeochemistry analysis were taken from core catchers
161 originating from hole 5041-1B. Immediately after core retrieval, mini cores were taken from
162 the core catchers using pre-cut and autoclaved syringes for microbial analyses. These
163 minicores were then stored at -12 °C until further processing. The ages of the core catcher
164 sediment samples of core 5045-1B were inferred from the published age model [1].

165

166

167 3.2. Sediment chemistry

168

169 Biogeochemical data of core catcher samples presented herein were previously published
170 [34]. After freeze-drying, total carbon (TC) and total inorganic carbon (TIC) were analyzed as
171 released CO₂ from powdered material using an DIMATOC 200 (DIMATEC Co.) TOC was
172 calculated as the difference between TC and TIC. Total nitrogen (TN) concentrations were
173 analysed using a Vario MicroCube for this study.

174 X-ray fluorescence (XRF) analyses were carried on freeze-dried, powdered aliquots (1 g) of the
175 core catcher samples using an ITRAX core scanner (Cox Analytical). The ITRAX core scanner
176 was equipped with a chromium (Cr) X-ray source and was run at 30 kV and 30 mA, with an
177 integration time of 10 s. Data processing was performed with the QSpec 6.5 software (Cox
178 Analytical).

179 Magnetic property data were taken from Just et al. (2016). Climatic data (including simulated
180 precipitation and temperatures) were taken from Wagner et al. (2019).

181

182 3.3. DNA extraction and sequencing

183

184 Half a cm³ of wet sediment was extracted for each sample, using the MOBIO powersoil
185 extraction kit by Qiagen. We realized triplicate DNA amplification of ca. 10 ng of DNA per
186 triplicate using universal primer 515F (5'-GTGYCAGCMGCCGCGGTA-3') and 909R (5'-
187 CCCCYCAATTCMTTTRAGT-3') for the V4- V5 hypervariable region of the 16S rRNA gene [39],
188 with indexes integrated following the dual-indexing procedure described by Kozich et al.
189 (2013). Pooled triplicate products were then quantified and using Picogreen assay (Life
190 Technologies) and pooled equimolarly (same amount for each sample). The final pool was
191 concentrated with SpeedVac Plus SC110A Savant and purified with CleanNA beads (Moka

192 science) before sequencing was realized by Fasteris (Geneva, Switzerland) on an Illumina
193 Miseq with 2 × 250 cycles, with settings of 7.5 Gb yield (including PhiX), an error rate of 2.5%
194 and Q30 at 75%.

195

196 3.5. DNA sequences processing

197

198 The final analysis error rates were within quality specifications. The workflow included
199 adapters removal using trimmomatic [41], paired-ends reads joining with ea-utils [42], quality-
200 check using FastQC, and samples demultiplexing by Fasteris in-house script. 16S rRNA gene
201 sequences were then processed using Mothur [43]. Samples were dereplicated, aligned, and
202 filtered by length. Chimeras were removed using uchime [44], and taxonomic affiliation was
203 then realized using the method of [45] at a cutoff of 80% against the Silva SSU database 123
204 [46]. Known common contaminants were removed based on the list provided by Sheik et al.
205 (2018). Operational Taxonomic Units (OTU) were then defined at a 97% similarity and used
206 for similarity analysis. Random subsampling was realized based on the smallest number of
207 obtained sequences in one sample after singleton removal.

208 All alpha-diversity indexes were calculated based on OTU matrix using Mothur. The beta-
209 diversity indexes (Local Contribution and Species Contribution to β -diversity) were calculated
210 from the same matrix with R using formula provided by Legendre and De Cáceres (2013).

211

212 3.6. Data analysis

213

214 All community composition plots and multivariate analyses presented in this article were
215 realized using the decontaminated relative composition based on 16S rRNA gene sequence
216 taxonomy at the phylum level. Diversity profiles were obtained using the decontaminated
217 OTU list using Mothur [43]. Two matrixes (sample vs microbial composition relative
218 percentage at the phylum level and sample vs normalized OTU distribution) were constructed
219 and Principal Coordinate Analyses were run.

220 Three matrices were built for multivariate analyses of sedimentary and community
221 composition (Principal Component Analysis and Canonical Correlation Analysis). To present
222 environmental variables, such data were pooled into 3 different matrixes (lithology, magnetic
223 properties and simulated climatic variables), normalized and a principal component analysis

224 was obtained using the software PAST [49]. The matrixes were then normalized by subtracted
225 means and compared with a matrix of the relative percentage of each phylum using a CCA
226 with 999 permutations on PAST. The same comparison was conducted with a normalized
227 community matrix at the OTU level. ANOSIM tests were then run to test for the significance
228 of each parameter with the community composition.

229 Finally, potential functions were obtained using the online tool METAGENassist [50] based on
230 taxonomic affiliation of obtained OTUs. A heatmap was built using Pearson distance and Ward
231 clustering algorithm after unmapped and unassigned reads were excluded, along with OTUs
232 appearing in only 10% of the samples. Data filtering was done using interquartile range. Row-
233 wise (sample by sample) normalization was performed using the median, while column-wise
234 normalization was done by auto-scaling (mean-centered and divided by the standard
235 deviation for each variable).

236 The matrices are available in supplementary material, and the complete list of OTUs and
237 sequences can be downloaded from NCBI Genbank (MT066494 - MT067558) and on the Open
238 Science Framework data repository (<https://osf.io/s9e2q/>).

239

240 4. Results

241

242 4.1. Lake and sediment characteristics

243

244 Due to the low sampling resolution, sedimentary characteristics display a relatively scattered
245 pattern along depth (Fig. 2), but conserve a strong relationship with climatic patterns (warm
246 vs cold periods) (Fig. 3). A plot of the principal components explaining 62 + 13 % of the variance
247 shows that TIC and Ca vary together (Fig. 3). TOC and the C/N ratio also have a similar
248 behavior. Detrital elements Ti, K, Al and Si are anticorrelated to TOC. Fe, As and Mn have quite
249 similar behavior with each other, but seem not correlated to sediment depth. Overall, there
250 is a marked distinction between samples that have high TOC, C/N ratio, Ca and TIC, and others
251 that have higher Mn, As, Fe, Ti, K, Al and Si values. The former mainly belong to interglacial
252 stages, while the second are generally from glacial periods. Three remarkable samples can be
253 identified based on their environmental parameters' characteristics: the samples at 191.9 and
254 29.1 m, which have high Fe/Mn ratio values, and the sample at 4.7 m, which has low Fe/Mn
255 and high As and Mn.

256 Magnetic properties have been described in detail in Just et al. (2016). The displayed PCA here
257 explains 28+38 % of the variance (Fig. 3). Magnetic susceptibility (κ) and hard Isothermal
258 remanent magnetization behave similarly. They show a slight anticorrelation with depth. The
259 other properties seem independent from each other. No clear cluster can be observed for the
260 samples. Samples between 4.7 and 29.1 m are characterized by high κ and HIRM. The
261 shallowest sample, at 1.8 m, is rather characterized by a high S ratio and high saturation
262 isothermal remanent magnetization (SIRM). Samples below 95.8 m bear a higher imprint of
263 greigite, marked by high $\Delta\text{GRM}/\Delta\text{NRM}$. No clear distinction is observed in terms of glacial vs
264 interglacial stages.

265

266 4.2. Microbial community composition and variation

267

268 The number of reads obtained from the profile varies largely and has to be taken into account
269 when analyzing the structure of the community. Reads drop significantly with depth, in
270 particular below 60 m (Fig. 2). This distribution is correlated with the decrease in the number
271 of taxa (OTUs), although it is not exactly similar. However, diversity indexes are not related to
272 read numbers. Evenness steadily increases with depth, but the Shannon index remains quite
273 high all along the 200 m of profile, and only drops below 4 at 95.8 m and 201.9 m. Otherwise,
274 it remains close to 4.5 and even 5 throughout the core. Local contribution to beta diversity
275 peaks at 9.6 m in association with an increase of evenness. It then sharply decreases and
276 follows a general increasing trend with depth, with a second maximum at 95.8 m correlated
277 to high dominance and minimum evenness.

278 Based on PCoA results, three main phyla seem to significantly drive the structure of the deep
279 biosphere community (Fig. 4): *Bathyarchaeota*, *Atribacteria* and *Betaproteobacteria*. They are
280 all uncorrelated to each other and vary independently. Other obtained phyla that show
281 significant relative percentages are *Alphaproteobacteria*, *Dehalococcoidia*, members of
282 *Actinobacteria* group OPB41, and to a lesser extent, *Physisphaerae*, *Gammaproteobacteria*,
283 *Cyanobacteria*, *Bacteroidetes* and *Acidobacteria* (Fig. 5). Two samples are marked by a high
284 relative abundance of *Betaproteobacteria* members: 9.6 m and 147.9 m (Figs. 5 and 6).
285 *Cyanobacteria* are also abundant in these layers. *Atribacteria* abundance increases with
286 depth, while *Bathyarchaeota* and *Dehalococcoidia* vary a lot with depth (Fig. 6). No clear
287 cluster is observable regarding community composition along the profile. Samples from glacial

288 intervals at 7.2, 12.4, 19.1, 54.3 and 68.8 m have similar compositions to samples from
289 interglacial or transitional intervals at 1.8, 4.7, 39.9 and 95.8 m (Fig. 4). Species contribution
290 to beta-diversity is mostly carried by OTUs associated to *Bathyarchaeota* (39% of the first 40
291 OTUs), with *Atribacteria* (9%), *Gammaproteobacteria* (9%) and Clostridia (8%) having an
292 important contribution too (Fig. 7).

293 Results from METAGENassist analyses only allowed assigning functions to a rather small
294 percentage of OTUs (25% for metabolisms). They show that samples at 7.2, 9.6 and 12.4 m
295 have a higher proportion of organisms associated to aquatic habitats. Higher sporulation is
296 observed for deep samples at 109.5, 179.4, 191.9 and 201.9 m, along with enhanced motility
297 (147.9, 191.9 and 201.9 m). Just like diversity, large variations are observed for metabolisms
298 (Fig. 8). Sulfate reducer and sulfide oxidizers dominate between 12.4 and 29.1 m, and in
299 samples at 54.3 m. Dehalogenation follows a similar occurrence. Sulfate reducers are also
300 largely present at 95.8 m with nitrite reducers. Sulfide reducers are dominant at 134.7 m,
301 along with N fixators and nitrite reducers. CO₂ fixation seems to dominate in the deep layers
302 at 147.9, 164.8 and 201.8 m. Hydrogen production is always associated to this CO₂ fixation.
303 Outlier sample at 9.6 m is dominated by aromatic hydrocarbon degradation, sulfur oxidation
304 and metabolizing organisms. Sulfur metabolizing functions are also dominant at 1.8 m and
305 39.9 m. Finally, methanogenic functions are observed between 12.4 and 39.9 m, and dominate
306 particularly at 19.1 m.

307 We plot a canonical correlation analysis of a selection of these parameters (excluding
308 magnetic properties) against microbial community composition at the phylum level (Axis 1:
309 38.56 % of variance, axis 2: 29.4 % of variance; Fig. 9). We observe a rough anti-correlation
310 between phyla *Alphaproteobacteria*, *Betaproteobacteria* and *Cyanobacteria* with TOC content
311 and simulated precipitation. *Actinobacteria* OPB41, *Gammaproteobacteria* and *Atribacteria*
312 seem to increase relatively with depth and age of the sediment, unlike *Phycisphaerae*,
313 *Anaerolineae* or *Deltaproteobacteria*. However, multivariate analysis comparing environmental
314 parameters and phyla or OTU matrix did not yield significant results based on ANOSIM tests
315 ($p > 0.05$), and therefore all tested hypotheses of a significant influence of environmental
316 parameters (magnetic properties, sedimentary composition or simulated climatic variations)
317 on microbial diversity were rejected.

318

319 5. Discussion

320

321 5.1 Dominant taxa and associated metabolisms in the deep Ohrid sediment

322

323 Lake Ohrid sediments bear an original and diverse subsurface microbial community, based on
324 the analysis of 16S rRNA gene sequences (Figs. 2 and 5). Three main phyla have been
325 identified, two from the bacterial domain and one from the archaeal domain (Fig. 5).
326 *Betaproteobacteria* seem to play a significant role in the structuration of the subsurface
327 community and are mainly occurring in two specific samples that largely differ from the others
328 (i.e. 9.6 m, and 147 m; Fig. 5). These two samples have different taxonomic compositions
329 resulting in different results in terms of metabolic prediction (Fig. 8). While the 9.6 m sample
330 seems to be dominated by naphtalene, chitin and aromatic hydrocarbon degradation, along
331 with sulfur related metabolisms (potentially sulfur oxidizers), the 147 m sample mainly
332 exhibits hydrogen production and carbon dioxide fixation. Such metabolisms are common in
333 low energy deep biosphere samples, where phyla like *Atribacteria* produce H₂ as a
334 fermentative product [51]. The 9.6 m sample seems to be dominated by an oxic habitat
335 community (as suggested by the varied organic matter degradation metabolic capacities
336 outlined by METAGENassist, Fig. 8). As a consequence, we suggest that most of the DNA
337 extracted from this sample associates with high amounts of terrestrial OM thereby likely also
338 containing soil microbes masking the subsurface biosphere contribution in this level.
339 Conversely, this sample exhibits minimum TOC that could coincide with oxidative conditions
340 at the time of deposition [2]. Hence, we suggest preservation of ex-situ microbial DNA rather
341 than this sample being representative for an in situ sedimentary microbial community.

342 The two other most significant phyla observed in Ohrid sediments belong to the archaeal
343 candidate division *Bathyarchaeota* and the bacterial division *Atribacteria*. These are both
344 common phyla in sedimentary environments at depth [52], and particularly in the marine
345 realm [e.g. 32], where their occurrence has been associated with strong adaptations to low
346 energy environments and varied fermentative abilities. *Atribacteria* have been suggested to
347 perform primary fermentation of carbohydrates and secondary fermentation of organic acids
348 (propionate among others), leading to the production of H₂ [32,51]. *Bathyarchaeota* are more
349 enigmatic as they have been hypothesized as organoheterotrophic and autotrophic acetogens
350 [53], potentially able to perform dissimilatory nitrite reduction to ammonium. Lloyd et al.
351 (2013) also suggested they could degrade detrital proteins. Finally, CH₄ production was also

352 hypothesized for this clade [55]. These two phyla appear as the most important contributors
353 to beta diversity among the 40 first OTUs contributions to SCBD (Fig. 7). They likely bear a
354 strong role in the deep subsurface of Lake Ohrid and are often associated with
355 *Dehalococcoidia* phylum sequences, which form a common deep biosphere clade, in particular
356 in marine sediments. Kawai et al. (2014) hypothesized anaerobic respiration of organohalides
357 for the *Chloroflexi* clade, but their catabolic reductive dehalogenation ability has been
358 questioned by the study of several assembled genomes, which suggested they had a strictly
359 anaerobic organotrophic or lithotrophic lifestyle. Sewell et al. (2017) suggested their
360 involvement in reductive dehalogenation with H₂ as an electron donor and linked them to
361 homoacetogenic *Chloroflexi*, which could connect their activity to other deep biosphere taxa
362 like H₂ producers *Atribacteria*, often presented as syntrophs [51] and potentially to
363 acetoclastic methanogens. Samples that have high *Atribacteria* and *Bathyarchaeota* relative
364 abundance often bear reads associated to *Deltaproteobacteria*, *Aminicenantes* and
365 *Bacteroidetes* (Figs. 4 and 5). Their metabolic abilities cannot be easily constrained using our
366 method, but their occurrence has often been acknowledged in the deep subsurface [32].
367 Potential association with sugar fermentation coupled with Mn and Fe reduction was
368 hypothesized for *Bacteroidetes* members [see in 32], but this does not come out in our
369 METAGENassist simulation (Fig. 8). However, they likely have energy conservative
370 metabolisms allowing them to remain present in extreme deep lacustrine sediments [25].
371 Based on sedimentary intracellular DNA analysis, *Deltaproteobacteria*, *Bathyarchaeota* and
372 *Clostridia* were shown to be part of the growing communities with depth in ferruginous Lake
373 Towuti, suggesting they are well adapted to the deep subsurface environment [58].
374 Based on our METAGENassist simulation (Fig 8), samples between 12.4 to 29.1 m and at 54.3
375 m carry a strong similarity in metabolic potential, encompassing ammonia oxidation,
376 dehalogenation (likely supported by *Dehalococcoidetes*), sulfate reduction, sulfide oxidation,
377 xylan degradation and methanogenesis. All metabolisms seem hard to conjugate in one single
378 sample, as some are strictly anaerobic while others require oxygen. Apart from the fact that a
379 major fraction of observed OTUs could not be linked to any functional potential, it is likely that
380 our METAGENassist simulation is biased by the contribution of archived sedimented DNA from
381 the catchment and water column. It could be the case of soil derived *Acidobacteria*, or water
382 derived *Alphaproteobacteria* or *Physisphaera* for example. The contribution of
383 *Betaproteobacteria* and *Cyanobacteria* suggests likewise.

384

385 5.2 Diversity changes along depth

386

387 Observations of diversity changes from the most significant taxa fails to exhibit a clear pattern
388 along depth. Except for *Atribacteria* (Fig. 6), *Gammaproteobacteria* and OPB41 (Fig. 8) that
389 tend to increase in relative abundance with depth (below 10 m), the relative abundance of
390 common deep subsurface taxa such as *Bathyarchaeota* or *Dehalococcoidia* does not exhibit a
391 clear trend. This is reflected in the varied alpha and beta-diversity indexes used (Fig. 2).
392 Regardless of the number of OTUs, Shannon index remains relatively high although a gentle
393 decrease is observed with depth and corresponds likely with an increase of evenness that
394 should be associated to the increasing contribution of energy-conservative taxa. Decrease of
395 read number also suggests biomass and DNA quality decrease with depth. This is similar to
396 the diversity profiles observed down to 80 m in freshwater lake Laguna Potrok Aike [25].
397 However it is worth noticing that this diversity is lower compared to what has been observed
398 in shallow lake sediments (first m) [e.g. 31,59]. Local contribution to beta diversity is very high
399 for the sample at 9.6 cm, as expected given its peculiarity in microbial community. Below 40
400 m, a general increase can be observed towards the deepest layers, that could be associated
401 to a general depletion of less adapted taxa and a relative increase in the low-energy taxa such
402 as *Bathyarchaeota* members, which carry much of the SCBD. Going deeper, we conclude that
403 we tend to lose the diversity that has been provided by the sedimenting DNA in paleolake
404 Ohrid. Low energy, well adapted slow growers common in deep subsurface environments
405 necessarily take over in terms of relative abundance, as described by Kirkpatrick et al. (2019)
406 in the marine realm, or Wurzbacher et al. (2017) in higher depth of lake sediments. In the
407 deep sediments of Lake Ohrid, this pattern is roughly carried by *Atribacteria* and OPB41 (Fig.
408 9). These two phyla are known to catabolize sugars, suggesting availability of this substrate
409 and their catabolic products with depth [61]. They were also shown to express several
410 subsistence mechanisms in deep environments. In particular, *Atribacteria* has the ability to
411 produce *de novo* amino acids and export them in very low energy environments, likely halting
412 cell growth and suggesting metabolic interdependencies [61]. *Gammaproteobacteria* relative
413 abundance also seems to increase with age or depth of the sediment, but the poor taxonomic
414 affiliation of members of this genus prevents any further interpretation on this basis.

415

5.3 Impact of environmental parameters on current communities

416
417

418 Multivariate analyses coupled with ANOSIM tests failed to identify specific external
419 parameters that were significantly linked to given OTU or phyla relative abundance. We can
420 however identify some covariance based on Fig. 9. In particular, *Atribacteria* and OPB41
421 members were identified as being increasingly dominant with depth. Metatranscriptomics,
422 metabolomics and single cell genomics studies from deep sediments of the Baltic Sea have
423 highlighted the adaptations and metabolic activity allowing *Actinobacteria* group OP41 and
424 *Atribacteria* to remain active in low energy environments like the deep sediments of Lake
425 Ohrid [61].

426 Samples between 12.4 to 29.1 m and at 54.3 m are all from glacial intervals. They exhibit a
427 mix of metabolic potential involving anaerobic and aerobic processes (Fig. 8). While anaerobic
428 degradation processes coincide with sedimentary conditions, the presence of sequences
429 associated to aquatic habitats, xylan degraders, N-fixers, *Betaproteobacteria* and
430 *Cyanobacteria* fits quite well with the Ohrid depositional model in which glacials are
431 characterized by lower productivity and enhanced input of soil sediments from the catchment.
432 This also coincides with low TOC, TIC and C/N levels, that have been associated to glacial
433 stages with lower productivity and enhanced detrital inputs in Lake Ohrid [2,5]. Consequently,
434 the obtained DNA in these layers could result in a mix of archived sedimentary DNA, and active
435 OM anaerobic degraders.

436 Of special interest is the occurrence of *Cyanobacteria* in samples at 9.6 m dated at 24 ka and
437 at 147.9 m at 340 ka. As *Cyanobacteria* are not expected to be active in the deep sediment,
438 relative cyanobacterial increase in samples from glacial periods is likely associated to an
439 increase in archived fossil DNA. In temperate lakes, limited nutrient and in particular N-
440 deficiency has consensually been shown to support blooms of N-fixing *Cyanobacteria* [62,63].
441 This could explain the increased presence of *Cyanobacteria* in the 9.6 m and 147.9 m samples
442 of Lake Ohrid, along with low C/N ratio [64], since dry and cold conditions during glacial
443 periods likely caused nutrient depletion in Lake Ohrid [4]. However, most cyanobacterial
444 sequences obtained from these intervals could not be affiliated to a given genus, and those
445 that were affiliated mainly belong to *Cyanobium*, which seems to lack N-fixing genes [65].
446 Some work on fossil sedimentary DNA possibly dovetailed with characteristic pigment analysis

447 could therefore reveal information on the evolution of Lake Ohrid's productivity and
448 planktonic communities in relation with Quaternary changes of nutrient availability.

449

450 5.4 Lake Ohrid specificity

451

452 Lake Ohrid is characterized by marked changes in sedimentary composition between glacial
453 and interglacial periods [2,13][2], which contribute to the use of the Lake Ohrid sedimentary
454 record for powerful paleoclimatic reconstructions [e.g. 1]. However, the study of the lake
455 biosphere also highlights the strong resilience of the planktonic to benthic communities to
456 major climatic events [14,15]. Based on our DNA data, the behavior of the deep biosphere and
457 the parameters controlling their diversity are quite complex to disentangle. First of all, the
458 limits of the environmental data available are significant. While bulk sedimentary XRF and
459 magnetic data can provide key information regarding sedimentary processes at a macroscale,
460 they lack the second order precision that could help unravel early diagenetic processes, which
461 could be better addressed using for example pore water chemistry and stable isotope
462 composition.

463 Links with changes in diagenetic conditions, identified by Just et al. (2016), could not be
464 confirmed. Based on a difference in early diagenetic precipitates (shifts from ferrimagnetic
465 iron sulfides to siderites at 320 ka, ca. 140 m), the authors suggested higher sulfate
466 concentration in the lake before 320 ka. This would have permitted a deeper penetration of
467 sulfate in the sediment and favored formation of iron sulfide via sulfate reduction. After 320
468 ka, rapid depletion of sulfate in the shallow sediments of the lake may have permitted the
469 formation of siderite through methanogenesis dominance in the shallow sediments. We
470 observe a general peak in the presence of potential sulfate reducers between 30.83 ka and
471 316.43 ka (although samples at 39.9, 68.8 83.5 and 109.5 m do not bear this signal). Before
472 320 ka, no peak in potential sulfate reducers nor methanogens could be identified. Moreover,
473 no obvious dichotomy between methane-driven vs sulfur-driven cycling in the 16S rRNA gene
474 composition of the sediments were observed. This can be due either to a suppression of the
475 potential methanogenic or sulfate reducer genetic signatures with time. The sulfate-methane
476 transition zone is indeed generally constrained to the first centimeter of the sediment [31,32]
477 and while some signatures could be retained with burial [24], the continued microbial activity
478 in the deep sediment may lead to turnover of the dominant communities and overall

479 suppression of the initial signal. We may also miss their presence through the use of non-
480 specific 16S rRNA gene sequencing. Targeting and quantifying functional genes associated to
481 sulfate reduction (*dsrA*) or methanogenesis (*mcrA*) in the archived DNA pool of the deep Ohrid
482 sediment could provide valuable insights on this question.

483 Interestingly, samples older than 320 ka indeed support different metabolic potential than
484 younger ones. In particular, hydrogen production and carbon dioxide fixation are the main
485 metabolisms highlighted by our simulation (Fig. 8). The extent to which this might be related
486 to a change in cycling from sulfate- to methane-driven microbial cycling in the first place
487 remains unresolved. Potential microbial OM consumption by sulfate reduction and
488 subsequent fermenting processes may have depleted OM to a more important extent than in
489 methane-driven microbial communities. The lack of labile OM available as a carbon source for
490 deep sedimentary communities below 135 m may lead to a shift towards more dominant
491 chemolithoautotrophic metabolisms. The conjunction of H₂ production along with CO₂
492 fixation directs towards a potential niche for hydrogenotrophic methanogenesis or
493 acetogenesis. Such processes have been suggested in the past for deep lacustrine sediments
494 [66] and deep marine sediments and hydrothermal systems [67,68].

495 Intracellular vs extracellular DNA extraction methods have shown their value in the study of
496 deep life in lacustrine settings [58]. Such methods could confirm that *Cyanobacteria* and
497 *Betaproteobacteria*, significantly influencing the compositions of samples from 9.6 m and
498 147.9 m, are inherited from dead cell biomass. It would also allow discriminating between
499 transported-archived vs active-dormant living microbes in the deep sediment of Lake Ohrid,
500 since spore-forming or motility abilities seem to increase with depth.

501 Finally, a significant part of the community diversity is held by phylotypes adapted to low
502 energy environments, which suggests that Lake Ohrid deep biosphere is likely alive until ca.
503 515 ka ages (ca. 200 mblf), and that these phylotypes have partly erased a potential microbial
504 signature that could have been inherited through paleoclimatic conditions.

505

506 6. Conclusion

507

508 Based on 16S rRNA gene sequences, the subsurface biosphere composition of Lake Ohrid is
509 dominated by low energy microbial communities common to deep sedimentary settings,
510 regardless of their marine or lacustrine origin. *Bathyarchaeota*, *Atribacteria*, and

511 *Dehalococcoidia* play a strong role in structuring this subsurface community beta diversity.
512 The ability of these communities to adapt to low energy environments has likely erased the
513 potential original paleoenvironmental, paleolimnological and early diagenetic signals that
514 Lake Ohrid sediments have recorded, except for water column or soil DNA archiving during
515 dry glacial periods. Unlike other lacustrine systems, it seems that the strong resilience of Lake
516 Ohrid's ecosystem and/or the peculiar limnological characteristics of this lake basin do not
517 allow for the conservation or transfer of a specific microbial community in these sedimentary
518 archives.

519

520 References

521

- 522 1. Wagner, B.; Vogel, H.; Francke, A.; Friedrich, T.; Donders, T.; Lacey, J.H.; Leng, M.J.;
523 Regattieri, E.; Sadori, L.; Wilke, T.; et al. Mediterranean winter rainfall in phase with
524 African monsoons during the past 1.36 million years. *Nature* **2019**.
- 525 2. Francke, A.; Wagner, B.; Just, J.; Leicher, N.; Gromig, R.; Baumgarten, H.; Vogel, H.;
526 Lacey, J.H.; Sadori, L.; Wonik, T.; et al. Sedimentological processes and environmental
527 variability at Lake Ohrid (Macedonia, Albania) between 637 ka and the present.
528 *Biogeosciences* **2016**, *13*, 1179–1196.
- 529 3. Wagner, B.; Vogel, H.; Zanchetta, G.; Sulpizio, R. Environmental change within the
530 Balkan region during the past ca. 50 ka recorded in the sediments from lakes Prespa
531 and Ohrid. *Biogeosciences* **2010**, *7*, 3187–3198.
- 532 4. Wagner, B.; Lotter, A.F.; Nowaczyk, N.; Reed, J.M.; Schwalb, A.; Sulpizio, R.; Valsecchi,
533 V.; Wessels, M.; Zanchetta, G. A 40,000-year record of environmental change from
534 ancient Lake Ohrid (Albania and Macedonia). *J. Paleolimnol.* **2009**, *41*, 407–430.
- 535 5. Zanchetta, G.; Baneschi, I.; Francke, A.; Boschi, C.; Regattieri, E.; Wagner, B.; Lacey,
536 J.H.; Leng, M.J.; Vogel, H.; Sadori, L. Evidence for carbon cycling in a large freshwater
537 lake in the Balkans over the last 0.5 million years using the isotopic composition of
538 bulk organic matter. *Quat. Sci. Rev.* **2018**, *202*, 154–165.
- 539 6. Holtvoeth, J.; Vogel, H.; Valsecchi, V.; Lindhorst, K.; Schouten, S.; Wagner, B.; Wolff,
540 G.A. Linear and non-linear responses of vegetation and soils to glacial-interglacial
541 climate change in a Mediterranean refuge. *Sci. Rep.* **2017**, *7*, 1–7.
- 542 7. Holtvoeth, J.; Vogel, H.; Wagner, B.; Wolff, G. a. Lipid biomarkers in Holocene and

- 543 glacial sediments from ancient Lake Ohrid (Macedonia, Albania). *Biogeosciences* **2010**,
544 7, 3473–3489.
- 545 8. Just, J.; Nowaczyk, N.R.; Sagnotti, L.; Francke, A.; Vogel, H.; Lacey, J.H.; Wagner, B.
546 Environmental control on the occurrence of high-coercivity magnetic minerals and
547 formation of iron sulfides in a 640ka sediment sequence from Lake Ohrid (Balkans).
548 *Biogeosciences* **2016**, 13, 2093–2109.
- 549 9. Lacey, J.H.; Leng, M.J.; Francke, A.; Sloane, H.J.; Milodowski, A.; Vogel, H.;
550 Baumgarten, H.; Wagner, B. Mediterranean climate since the Middle Pleistocene: A
551 640 ka stable isotope record from Lake Ohrid (Albania/Macedonia). *Biogeosciences*
552 *Discuss.* **2015**, 12, 13427–13481.
- 553 10. Lacey, J.H.; Leng, M.J.; Francke, A.; Sloane, H.H.; Milodowski, A.; Vogel, H.;
554 Baumgarten, H.; Zanchetta, G.; Wagner, B. Northern Mediterranean climate since the
555 Middle Pleistocene: A 637 ka stable isotope record from Lake Ohrid
556 (Albania/Macedonia). *Biogeosciences* **2016**, 13, 1801–1820.
- 557 11. Leng, M.J.; Baneschi, I.; Zanchetta, G.; Jex, C.N.; Wagner, B.; Vogel, H. Late Quaternary
558 palaeoenvironmental reconstruction from Lakes Ohrid and Prespa
559 (Macedonia/Albania border) using stable isotopes. *Biogeosciences Discuss.* **2010**, 7,
560 3815–3853.
- 561 12. Reed, J.M.; Cvetkoska, A.; Levkov, Z.; Vogel, H.; Wagner, B. The last glacial-interglacial
562 cycle in Lake Ohrid (Macedonia/Albania): Testing diatom response to climate.
563 *Biogeosciences* **2010**, 7, 3083–3094.
- 564 13. Vogel, H.; Wagner, B.; Zanchetta, G.; Sulpizio, R.; Rosén, P. A paleoclimate record with
565 tephrochronological age control for the last glacial-interglacial cycle from Lake Ohrid,
566 Albania and Macedonia. *J. Paleolimnol.* **2010**, 44, 295–310.
- 567 14. Wagner, B.; Wilke, T.; Francke, A.; Albrecht, C.; Baumgarten, H.; Bertini, A.;
568 Combourieu-Nebout, N.; Cvetkoska, A.; D’Addabbo, M.; Donders, T.H.; et
569 al. The environmental and evolutionary history of Lake Ohrid (FYROM/Albania):
570 Interim results from the SCOPSCO deep drilling project. *Biogeosciences Discuss.* **2016**,
571 1–51.
- 572 15. Jovanovska, E.; Cvetkoska, A.; Hauffe, T.; Levkov, Z.; Wagner, B.; Sulpizio, R.; Francke,
573 A.; Albrecht, C.; Wilke, T. Differential resilience of ancient sister lakes Ohrid and
574 Prespa to environmental disturbances during the Late Pleistocene. *Biogeosciences*

- 575 **2016**, *13*, 1149–1161.
- 576 16. Föller, K.; Stelbrink, B.; Hauffe, T.; Albrecht, C.; Wilke, T. Constant diversification rates
577 of endemic gastropods in ancient Lake Ohrid: Ecosystem resilience likely buffers
578 environmental fluctuations. *Biogeosciences* **2015**, *12*, 7209–7222.
- 579 17. Baulch, H.M.; Schindler, D.W.; Turner, M.A.; Findlay, D.L.; Paterson, M.J.; Vinebrooke,
580 R.D. Effects of warming on benthic communities in a boreal lake: Implications of
581 climate change. *Limnol. Oceanogr.* **2005**, *50*, 1377–1392.
- 582 18. De Senerpont Domis, L.N.; Elser, J.J.; Gsell, A.S.; Huszar, V.L.M.; Ibelings, B.W.;
583 Jeppesen, E.; Kosten, S.; Mooij, W.M.; Roland, F.; Sommer, U.; et al. Plankton
584 dynamics under different climatic conditions in space and time. *Freshw. Biol.* **2013**, *58*,
585 463–482.
- 586 19. Zwirgmaier, K.; Keiz, K.; Engel, M.; Geist, J.; Raeder, U. Seasonal and spatial patterns
587 of microbial diversity along a trophic gradient in the interconnected lakes of the
588 Osterseen Lake District, Bavaria. *Front. Microbiol.* **2015**, *6*, 1–18.
- 589 20. Nam, Y. Do; Sung, Y.; Chang, H.W.; Roh, S.W.; Kim, K.H.; Rhee, S.K.; Kim, J.C.; Kim, J.Y.;
590 Yoon, J.H.; Bae, J.W. Characterization of the depth-related changes in the microbial
591 communities in Lake Hovsgol sediment by 16S rRNA gene-based approaches. *J.*
592 *Microbiol.* **2008**, *46*, 125–136.
- 593 21. Dong, H.; Jiang, H.; Yu, B.; Liu, X.; Zhang, C.; Chan, M.A. Impacts of environmental
594 change and human activity on microbial ecosystems on the Tibetan Plateau, NW
595 China. *GSA Today* **2010**, *20*, 4–10.
- 596 22. Ariztegui, D.; Thomas, C.; Vuillemin, A. Present and future of subsurface biosphere
597 studies in lacustrine sediments through scientific drilling. *Int. J. Earth Sci.* **2015**, *104*,
598 1655–1665.
- 599 23. Wilke, T.; Wagner, B.; Bocxlaer, B. Van; Albrecht, C.; Ariztegui, D.; Delicado, D.;
600 Francke, A.; Harzhauser, M.; Hauffe, T.; Holtvoeth, J.; et al. Scientific drilling projects
601 in ancient lakes: integrating geological and biological histories. *Glob. Planet. Change*
602 **2016**.
- 603 24. Vuillemin, A.; Ariztegui, D.; Leavitt, P.R.; Bunting, L. Recording of climate and
604 diagenesis through fossil pigments and sedimentary DNA at Laguna Potrok Aike,
605 Argentina. *Biogeosciences Discuss.* **2015**, *12*, 18345–18388.
- 606 25. Vuillemin, A.; Ariztegui, D.; Horn, F.; Kallmeyer, J.; Orsi, W.D. Microbial community

- 607 composition along a 50 000-year lacustrine sediment sequence. *FEMS Microbiol. Ecol.*
608 **2018**, 1–14.
- 609 26. Glombitza, C.; Stockhecke, M.; Schubert, C.J.; Vetter, A.; Kallmeyer, J. Sulfate
610 reduction controlled by organic matter availability in deep sediment cores from the
611 saline, alkaline Lake Van (Eastern Anatolia, Turkey). *Front. Microbiol.* **2013**, *4*, 1–12.
- 612 27. Thomas, C.; Ionescu, D.; Ariztegui, D. Impact of paleoclimate on the distribution of
613 microbial communities in the subsurface sediment of the Dead Sea. *Geobiology* **2015**,
614 *13*, 546–561.
- 615 28. Thomas, C.; Grossi, V.; Antheaume, I.; Ariztegui, D. Recycling of Archaeal Biomass as a
616 New Strategy for Extreme Life in the Dead Sea Deep Sediment. *Geology* **2019**.
- 617 29. Thomas, C.; Ebert, Y.; Kiro, Y.; Stein, M.; Ariztegui, D. Microbial sedimentary imprint
618 on the deep Dead Sea sediment. *Depos. Rec.* **2016**, 1–21.
- 619 30. Vuillemin, A.; Ariztegui, D.; Coninck, A.; Lücke, A.; Mayr, C.; Schubert, C. Origin and
620 significance of diagenetic concretions in sediments of Laguna Potrok Aike, southern
621 Argentina. *J. Paleolimnol.* **2013**, *50*, 275–291.
- 622 31. Wurzbacher, C.; Fuchs, A.; Attermeyer, K.; Frindte, K.; Grossart, H.-P.; Hupfer, M.;
623 Casper, P.; Monaghan, M.T.; Li, H.; Ettema, T.; et al. Shifts among Eukaryota, Bacteria,
624 and Archaea define the vertical organization of a lake sediment. *Microbiome* **2017**, *5*,
625 41.
- 626 32. Orsi, W.D. Ecology and evolution of seafloor and subseafloor microbial communities.
627 *Nat. Rev. Microbiol.* **2018**, *1*.
- 628 33. Matzinger, A.; Schmid, M.; Veljanoska-Sarafiloska, E.; Patceva, S.; Guseska, D.;
629 Wagner, B.; Müller, B.; Sturm, M.; Wüest, A. Eutrophication of ancient Lake Ohrid:
630 Global warming amplifies detrimental effects of increased nutrient inputs. *Limnol.*
631 *Oceanogr.* **2007**, *52*, 338–353.
- 632 34. Wagner, B.; Wilke, T.; Krastel, S.; Zanchetta, G.; Sulpizio, R.; Reicherter, K.; Leng, M.J.;
633 Grazhdani, A.; Trajanovski, S.; Francke, A.; et al. The SCOPSCO drilling project recovers
634 more than 1.2 million years of history from Lake Ohrid. *Sci. Drill.* **2014**, *17*, 19–29.
- 635 35. Leicher, N.; Zanchetta, G.; Sulpizio, R.; Giaccio, B.; Wagner, B.; Nomade, S.; Francke,
636 A.; Del Carlo, P. First tephrostratigraphic results of the DEEP site record from Lake
637 Ohrid (Macedonia and Albania). *Biogeosciences* **2016**, *13*, 2151–2178.
- 638 36. Meyers, P.A.; Ishiwatari, R. Lacustrine organic geochemistry-an overview of indicators

- 639 of organic matter sources and diagenesis in lake sediments. *Org. Geochem.* **1993**, *20*,
640 867–900.
- 641 37. Holtvoeth, J.; Vogel, H.; Wagner, T.; Wolff, G.A. Improved end-member
642 characterisation of modern organic matter pools in the Ohrid Basin (Albania ,
643 Macedonia) and evaluation of new palaeoenvironmental proxies Improved end-
644 member characterisation of modern organic matter pools in the Ohrid Basin (Alban.
645 *Biogeosciences* **2016**.
- 646 38. Vogel, H.; Wessels, M.; Albrecht, C.; Stich, H.B.; Wagner, B. Spatial variability of recent
647 sedimentation in Lake Ohrid (Albania/Macedonia). *Biogeosciences* **2010**, *7*, 3333–
648 3342.
- 649 39. Wang, Y.; Qian, P.Y. Conservative fragments in bacterial 16S rRNA genes and primer
650 design for 16S ribosomal DNA amplicons in metagenomic studies. *PLoS One* **2009**, *4*.
- 651 40. Kozich, J.J.; Westcott, S.L.; Baxter, N.T.; Highlander, S.K.; Schloss, P.D. Development of
652 a dual-index sequencing strategy and curation pipeline for analyzing amplicon
653 sequence data on the miseq illumina sequencing platform. *Appl. Environ. Microbiol.*
654 **2013**, *79*, 5112–5120.
- 655 41. Bolger, A.M.; Lohse, M.; Usadel, B. Trimmomatic: a flexible trimmer for Illumina
656 sequence data. *Bioinformatics* **2014**, *30*, 2114–2120.
- 657 42. Aronesty, E. ea-utils: Command-line tools for processing biological sequencing data.
658 *Expr. Anal. Durham, NC* **2011**.
- 659 43. Schloss, P.D.; Westcott, S.L.; Ryabin, T.; Hall, J.R.; Hartmann, M.; Hollister, E.B.;
660 Lesniewski, R. a; Oakley, B.B.; Parks, D.H.; Robinson, C.J.; et al. Introducing mothur:
661 open-source, platform-independent, community-supported software for describing
662 and comparing microbial communities. *Appl. Environ. Microbiol.* **2009**, *75*, 7537–7541.
- 663 44. Edgar, R.C.; Haas, B.J.; Clemente, J.C.; Quince, C.; Knight, R. UCHIME improves
664 sensitivity and speed of chimera detection. *Bioinforma.* **2011**, *27*, 2194–2200.
- 665 45. Wang, Q.; Garrity, G.M.; Tiedje, J.M.; Cole, J.R. Naïve Bayesian classifier for rapid
666 assignment of rRNA sequences into the new bacterial taxonomy. *Appl. Environ.*
667 *Microbiol.* **2007**, *73*, 5261–5267.
- 668 46. Quast, C.; Pruesse, E.; Yilmaz, P.; Gerken, J.; Schweer, T.; Yarza, P.; Peplies, J.;
669 Glöckner, F.O. The SILVA ribosomal RNA gene database project: improved data
670 processing and web-based tools. *Nucleic Acids Res.* **2013**, *41*, D590-6.

- 671 47. Sheik, C.S.; Reese, B.K.; Twing, K.I.; Sylvan, J.B.; Grim, S.L.; Schrenk, M.O.; Sogin, M.L.;
672 Colwell, F. Identification and removal of contaminant sequences from ribosomal gene
673 databases: Lessons from the Census of Deep Life. *Front. Microbiol.* **2018**, *9*, 840.
- 674 48. Legendre, P.; De Cáceres, M. Beta diversity as the variance of community data:
675 Dissimilarity coefficients and partitioning. *Ecol. Lett.* **2013**, *16*, 951–963.
- 676 49. Hammer, Ø.; Harper, D.; Ryan, P. PAST: Paleontological statistics software package for
677 education and data analysis. *Palaeontol. Electron.* **2001**, *4*, 9.
- 678 50. Arndt, D.; Xia, J.; Liu, Y.; Zhou, Y.; Guo, A.C.; Cruz, J.A.; Snelnikov, I.; Budwill, K.;
679 Nesbø, C.L.; Wishart, D.S. METAGENassist: a comprehensive web server for
680 comparative metagenomics. *Nucleic Acids Res.* **2012**, *40*, W88–W95.
- 681 51. Nobu, M.K.; Dodsworth, J.A.; Murugapiran, S.K.; Rinke, C.; Gies, E.A.; Webster, G.;
682 Schwientek, P.; Kille, P.; Parkes, R.J.; Sass, H.; et al. Phylogeny and physiology of
683 candidate phylum “Atribacteria” (OP9/JS1) inferred from cultivation-independent
684 genomics. *ISME J.* **2016**, *10*, 273–286.
- 685 52. Rinke, C.; Schwientek, P.; Sczyrba, A.; Ivanova, N.N.; Anderson, I.J.; Cheng, J.-F.;
686 Darling, A.E.; Malfatti, S.; Swan, B.K.; Gies, E. a; et al. Insights into the phylogeny and
687 coding potential of microbial dark matter. *Nature* **2013**, *499*, 431–437.
- 688 53. Lazar, C.S.; Baker, B.J.; Seitz, K.; Hyde, A.S.; Dick, G.J.; Hinrichs, K.U.; Teske, A.P.
689 Genomic evidence for distinct carbon substrate preferences and ecological niches of
690 Bathyarchaeota in estuarine sediments. *Environ. Microbiol.* **2016**, *18*, 1200–1211.
- 691 54. Lloyd, K.G.; Schreiber, L.; Petersen, D.G.; Kjeldsen, K.U.; Lever, M.A.; Steen, A.D.;
692 Stepanauskas, R.; Richter, M.; Kleindienst, S.; Lenk, S.; et al. Predominant archaea in
693 marine sediments degrade detrital proteins. *Nature* **2013**, *496*, 215–218.
- 694 55. Evans, P.N.; Parks, D.H.; Chadwick, G.L.; Robbins, S.J.; Orphan, V.J.; Golding, S.D.;
695 Tyson, G.W. Methane metabolism in the archaeal phylum Bathyarchaeota revealed by
696 genome-centric metagenomics. *Science (80-.)*. **2015**, *350*, 434–438.
- 697 56. Kawai, M.; Futagami, T.; Toyoda, A.; Takaki, Y.; Nishi, S.; Hori, S.; Arai, W.; Tsubouchi,
698 T.; Morono, Y.; Uchiyama, I.; et al. High frequency of phylogenetically diverse
699 reductive dehalogenase-homologous genes in deep seafloor sedimentary
700 metagenomes. *Front. Microbiol.* **2014**, *5*, 1–15.
- 701 57. Sewell, H, L.; Kaster, A.-K.; Spormann, A.M. Homoacetogenesis in Deep-Sea
702 Chloroflexi, as inferred by Single-Cell Genomics, Provides a link to Reductive

- 703 Dehalogenation in Terrestrial Dehalococcoidetes. *MBio* **2017**, *8*, 1–22.
- 704 58. Vuillemin, A.; Horn, F.; Alawi, M.; Henny, C.; Wagner, D.; Crowe, S.A.; Kallmeyer, J.
705 Preservation and Significance of Extracellular DNA in Ferruginous Sediments from
706 Lake Towuti , Indonesia. *Front. Microbiol.* **2017**, *8*, 1–15.
- 707 59. Wang, Y.; Sheng, H.F.; He, Y.; Wu, J.Y.; Jiang, Y.X.; Tam, N.F.Y.; Zhou, H.W. Comparison
708 of the levels of bacterial diversity in freshwater, intertidal wetland, and marine
709 sediments by using millions of illumina tags. *Appl. Environ. Microbiol.* **2012**, *78*, 8264–
710 8271.
- 711 60. Kirkpatrick, J.B.; Walsh, E.A.; D’Hondt, S. Microbial Selection and Survival in
712 Subseafloor Sediment. *Front. Microbiol.* **2019**, *10*, 1–15.
- 713 61. Bird, J.T.; Tague, E.D.; Zinke, L.; Schmidt, J.M.; Steen, A.D.; Reese, B.; Marshall, I.P.G.;
714 Webster, G.; Weightman, A.; Castro, H.F.; et al. Uncultured microbial phyla suggest
715 mechanisms for multi-thousand-year subsistence in baltic sea sediments. *MBio* **2019**,
716 *10*, 1–15.
- 717 62. Reynolds, C.S. Cyanobacterial Water-Blooms. *Adv. Bot. Res.* **1987**, *13*, 67–143.
- 718 63. Levich, A.P. The role of nitrogen-phosphorus ratio in selecting for dominance of
719 phytoplankton by cyanobacteria or green algae and its application to reservoir
720 management. *J. Aquat. Ecosyst. Heal.* **1996**, *5*, 55–61.
- 721 64. Teramoto, T.; Yoshimura, M.; Azai, C.; Terauchi, K.; Ohta, T. Determination of carbon-
722 to-nitrogen ratio in the filamentous and heterocystous cyanobacterium *Anabaena* sp.
723 PCC 7120 with single-cell soft X-ray imaging. *J. Phys. Conf. Ser.* **2017**, *849*, 3–7.
- 724 65. Scanlan, D.J.; Ostrowski, M.; Mazard, S.; Dufresne, A.; Garczarek, L.; Hess, W.R.; Post,
725 A.F.; Hagemann, M.; Paulsen, I.; Partensky, F. Ecological Genomics of Marine
726 Picocyanobacteria. *Microbiol. Mol. Biol. Rev.* **2009**, *73*, 249–299.
- 727 66. Vuillemin, A.; Ariztegui, D.; Nobbe, G.; Schubert, C.J. Influence of methanogenic
728 populations in Holocene lacustrine sediments revealed by clone libraries and fatty
729 acid biogeochemistry. *Geomicrobiol. J.* **2013**, *31*.
- 730 67. Amend, J.P.; McCollom, T.M.; Hentscher, M.; Bach, W. Catabolic and anabolic energy
731 for chemolithoautotrophs in deep-sea hydrothermal systems hosted in different rock
732 types. *Geochim. Cosmochim. Acta* **2011**, *75*, 5736–5748.
- 733 68. Lever, M.A.; Alperin, M.J.; Teske, A.; Heuer, V.B.; Schmidt, F.; Hinrichs, K.U.; Morono,
734 Y.; Masui, N.; Inagaki, F. Acetogenesis in Deep Subseafloor Sediments of The Juan de

735 Fuca Ridge Flank: A Synthesis of Geochemical, Thermodynamic, and Gene-based
736 Evidence. *Geomicrobiol. J.* **2010**, *27*, 183–211.

737

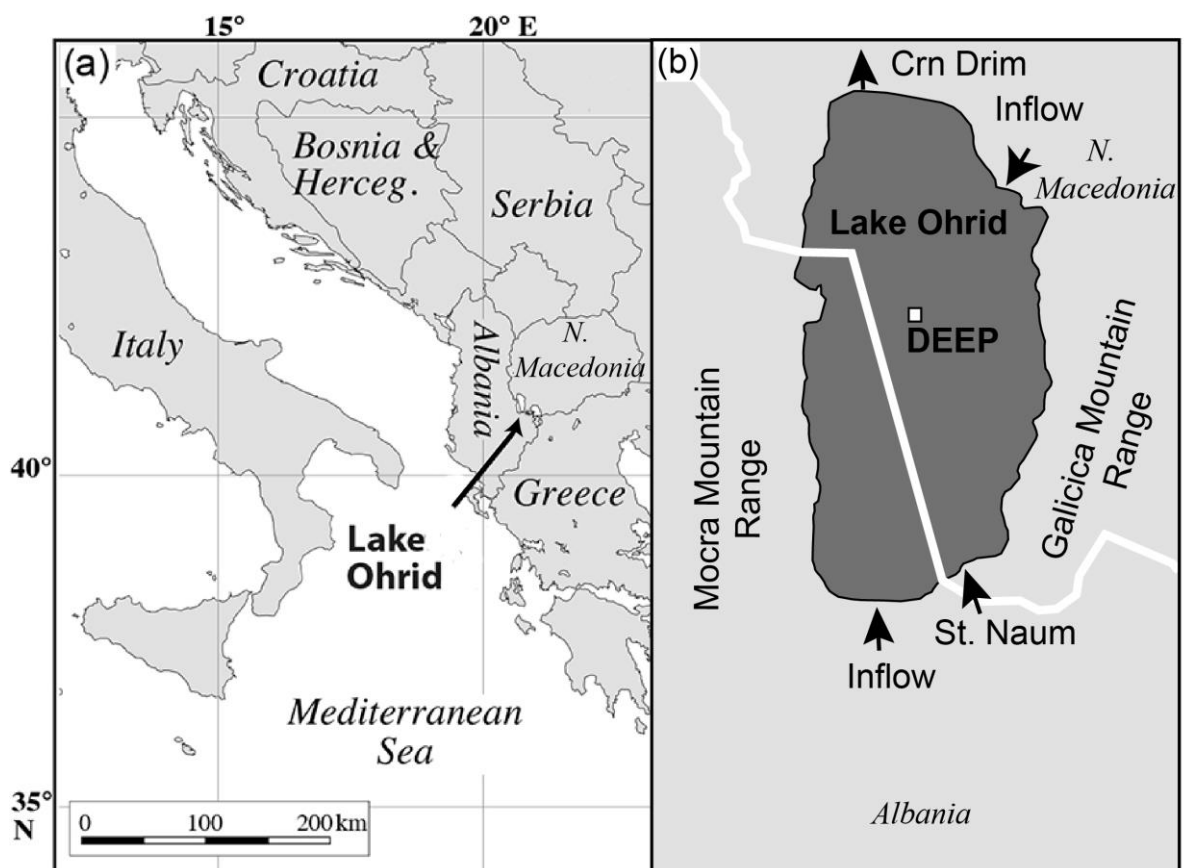
738

739 Figure and figure captions.

740

741 Fig. 1: Map of the location of Lake Ohrid (a), and of the DEEP drilling site (b) at the border
742 between N Macedonia and Albania.

743

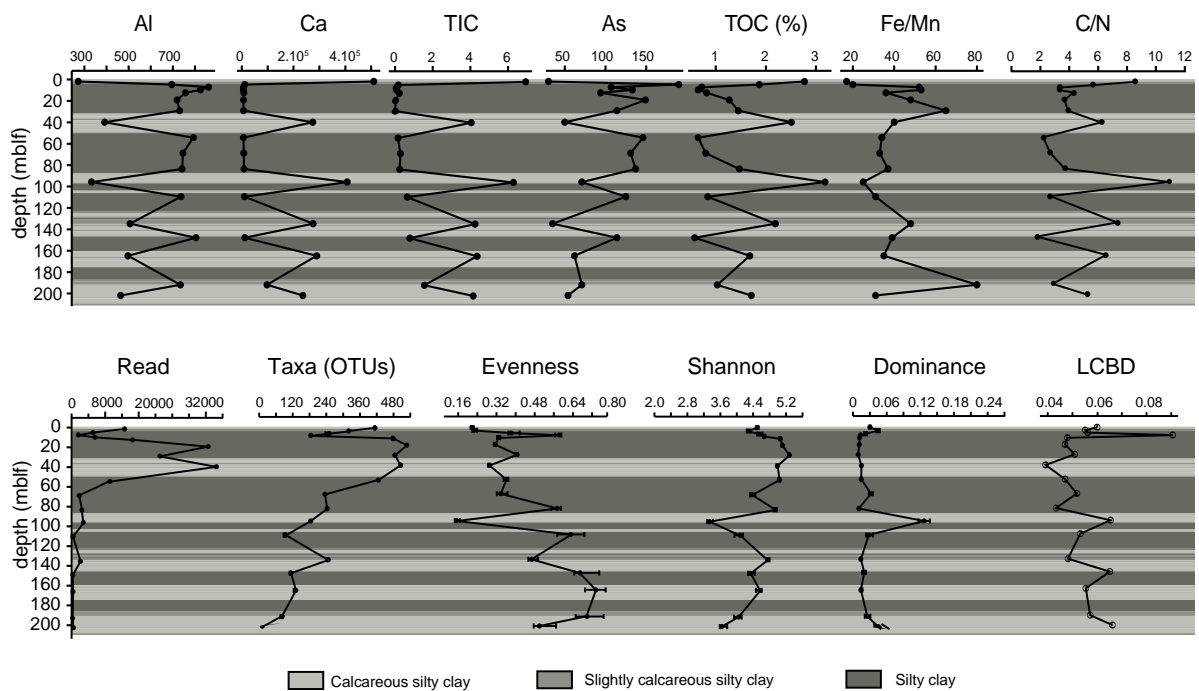


744

745

746 Fig. 2: Profiles of elemental composition and ratio along the core, with corresponding
747 sedimentary facies as described by Francke et al. (2016), and diversity profiles including
748 sequencing read number, OTU number, OTU richness, Shannon diversity index, evenness
749 and local contribution to beta diversity (LCBD) along the core.

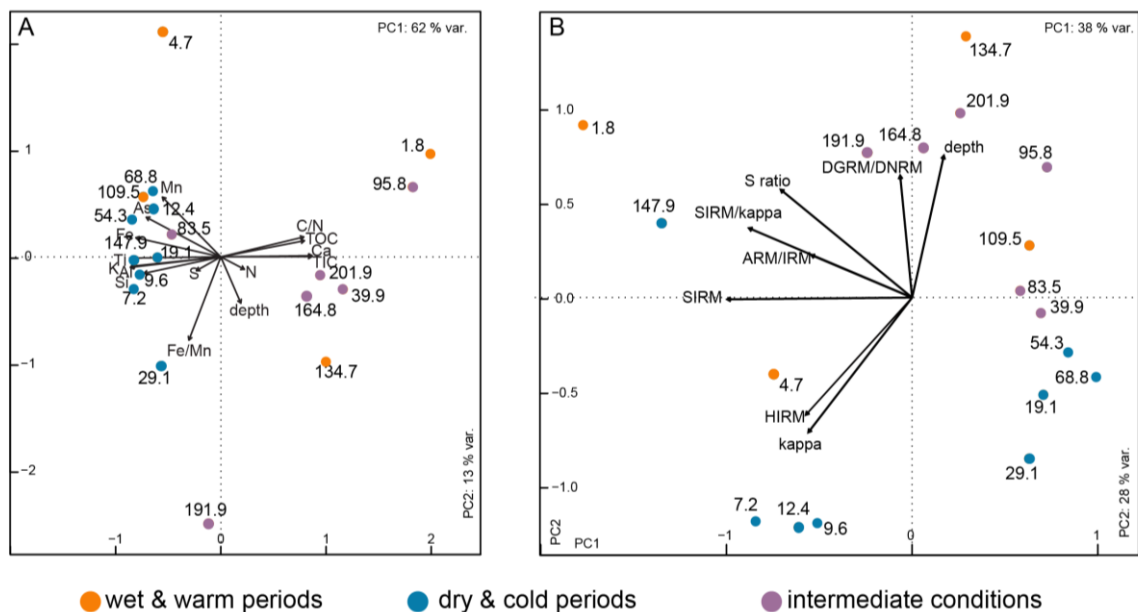
750



751

752

753 Fig. 3: Principal component analysis of elemental composition of the core (A) and magnetic
 754 properties (B) along the core. Numbers correspond to sample depth (in m), and colors code
 755 for wet and warm periods, mainly corresponding to interglacials (orange), dry and cold periods
 756 generally corresponding to glacial stages (blue), and intermediate conditions for transitional
 757 climatic stages (purple), based on data by [1,2,5,8]



758

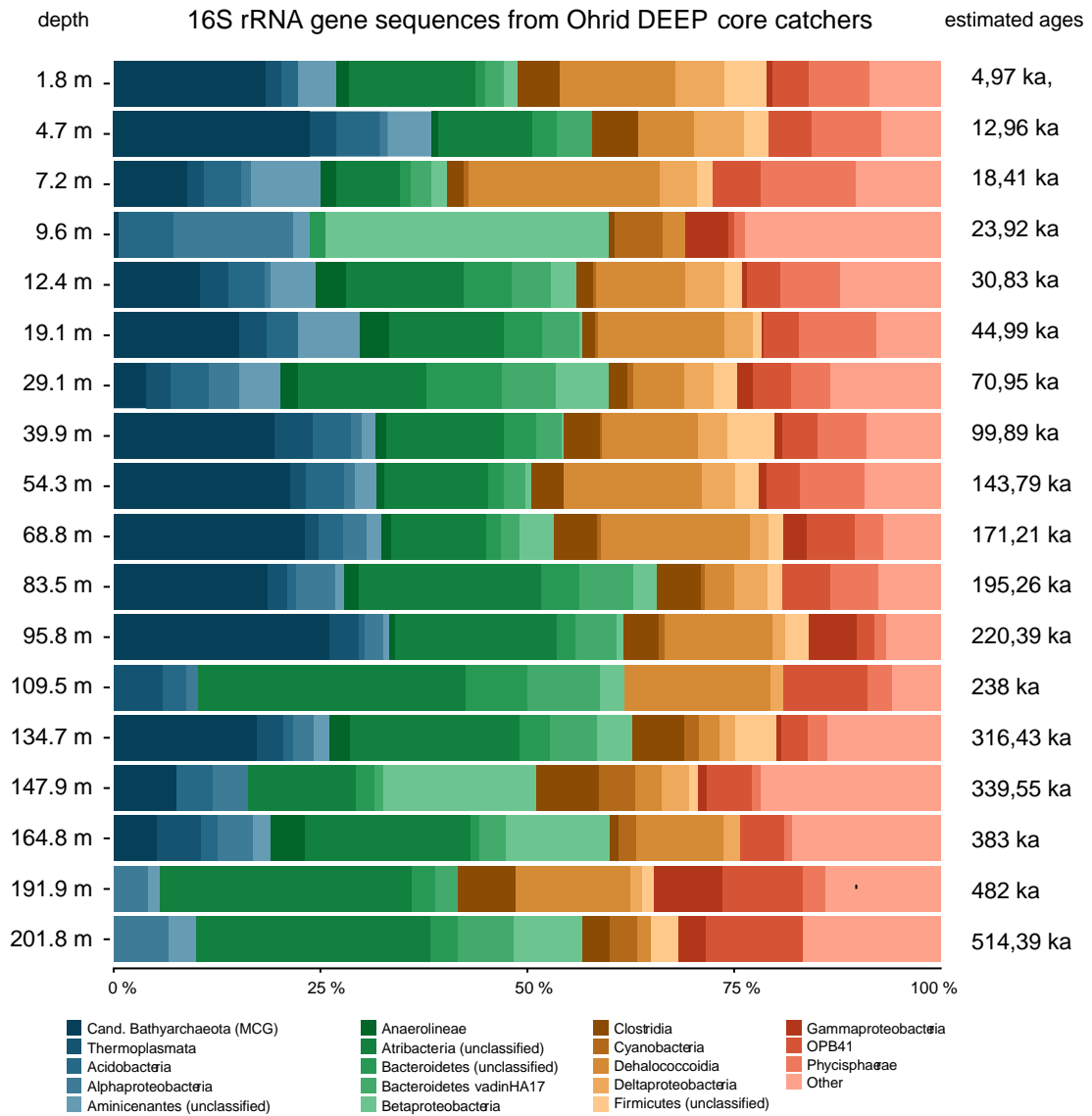
759

● wet & warm periods ● dry & cold periods ● intermediate conditions

760

761 Fig. 4: Relative abundance of 16S rRNA gene sequences per sample at the phylum level,
762 and corresponding estimated ages for each sample.

763



764

765

766

767

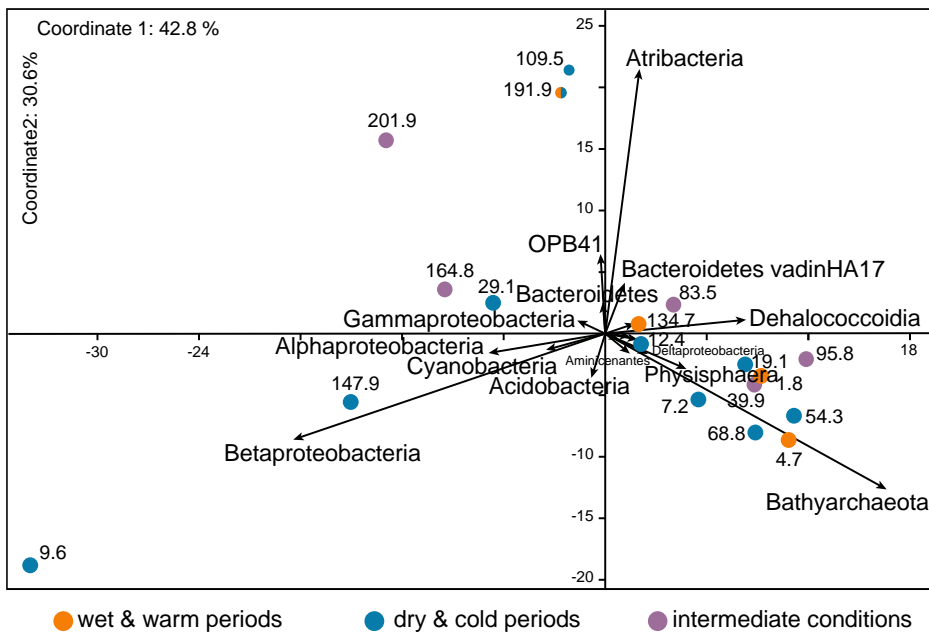
768 Fig. 5: Principal coordinate analysis of microbial community composition at the phylum level.

769 Colors code for wet and warm periods, mainly corresponding to interglacials (orange), dry and

770 cold periods generally corresponding to glacial stages (blue), and intermediate conditions for

771 transitional climatic stages (purple), based on data by [1,2,5]

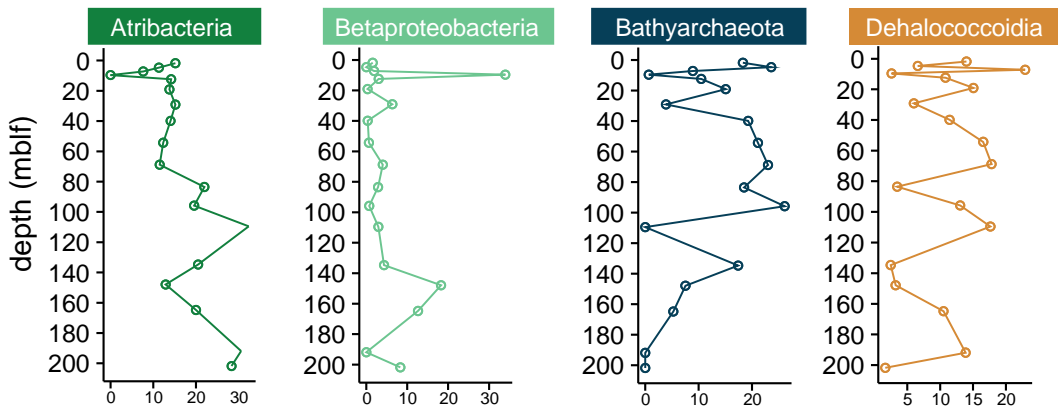
772



773

774

775 Fig. 6: Relative abundance profiles (read %) of the main microbial phyla along the core as
776 estimated by PCoA. Colors are the same as those used for Fig. 6.

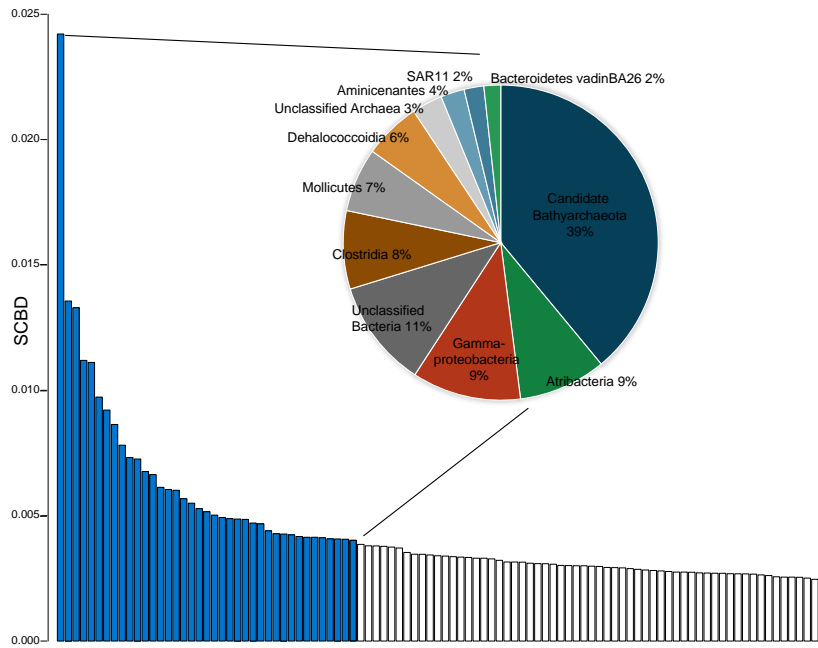


777

778

779 Fig. 7: Species contribution to betadiversity (SCBD) per OTU, and contribution and
780 taxonomic assignment of the 40 first OTUs. Colors are the same as those used in Fig. 4.

781

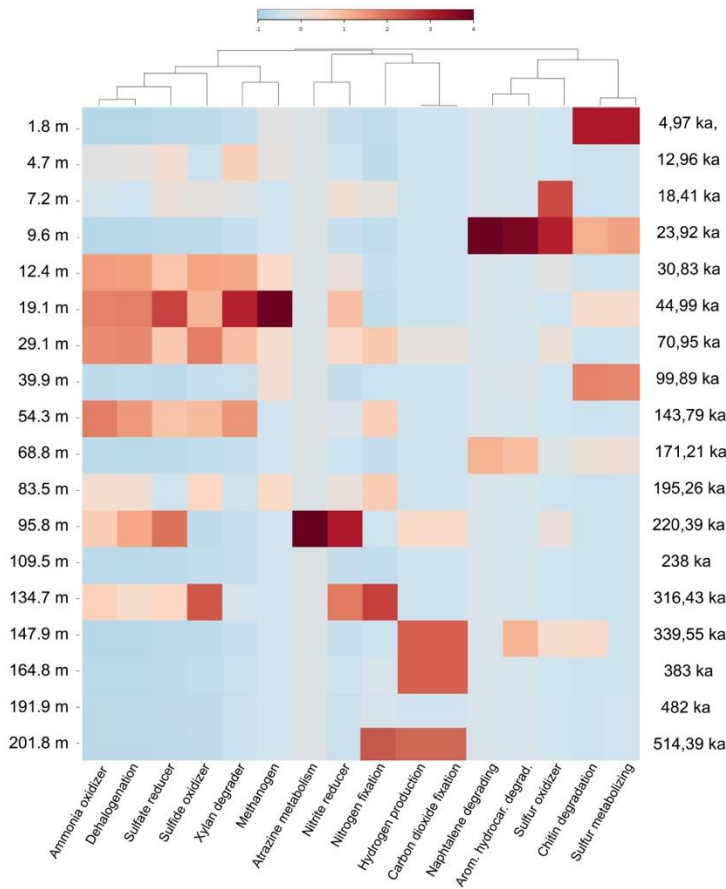


782

783

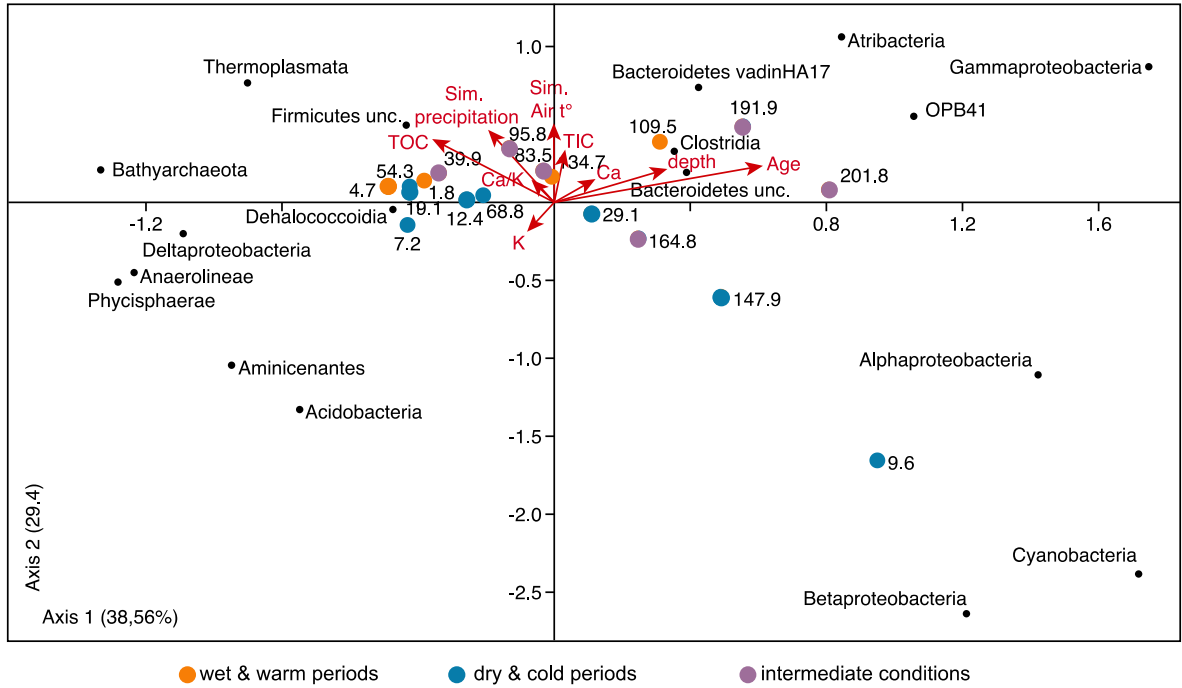
784 Fig. 8: Heatmap of potential metabolisms obtained from METAGENassist, with
 785 corresponding estimated ages.

786



787

788 Fig. 9: Canonical correlation analysis involving various paleoclimatically relevant proxy
 789 [1,2] and microbial phyla for the DEEP Ohrid sediment. Colors code for wet and warm
 790 periods, mainly corresponding to interglacials (orange), dry and cold periods generally
 791 corresponding to glacial stages (blue), and intermediate conditions for transitional climatic
 792 stages (purple).



793